THE INTERNATIONAL SOCIETY OF PRECISION AGRICULTURE PRESENTS THE
13th INTERNATIONAL CONFERENCE ON
PRECISION AGRICULTURE
July 31-August 4, 2016 • St. Louis, Missouri USA

Potential Improvement in Rice Nitrogen Status Monitoring using RapidEye and WorldView-2 Satellite Remote Sensing

Shanyu Huang[1,2],YuxinMiao[1*], Fei Yuan[3],Martin L. Gnyp[4], Yinkun Yao[1], Qiang Cao[5], Victoria Lenz-Wiedemann[1,2], Georg Bareth[1,2]

[1] International Center for Agro-Informatics and Sustainable Development (ICASD), College of Resources and Environmental Sciences, China Agricultural University, Beijing, China

[2] Institute of Geography, University of Cologne, 50923, Köln, Germany

[3] Department of Geography, Minnesota State University, Mankato, MN, 56001,USA

[4] Research Centre Hanninghof, Yara International, 48249 Duelmen, Germany

[5] National Engineering and Technology Center for Information Agriculture, Nanjing Agricultural University, Nanjing 210095, China

A paper from the Proceedings of the
13th International Conference on Precision Agriculture
July 31 – August 4, 2016
St. Louis, Missouri, USA

Abstract.*For in-season site-specific nitrogen (N) management of rice to be successful, it is crucially important to diagnose rice N status efficiently across large area in a timely fashion. Satellite remote sensing provides a promising technology for crop growth monitoring and precision management over large areas. The FORMOSAT-2 satellite remote sensing imageries with 4 wavebands have been used to estimate rice N status. The objective of this study was to evaluate the potential of using high spatial resolution satellites with red-edge band (RapidEye and WorldView-2) to improve monitoring rice N status in Northeast China. N rate experiments were conducted from 2008 thru 2009 and 2011 at Jiansanjiang, Heilongjiang Province of Northeast China. Field samples and hyperspectral data were collected at thepanicle initiation (PI), stem elongation (SE), and heading (HE)stages.Handheld hyperspectral data measured at canopy scale were used to simulate the wavebands of three satellite sensors-FORMOSAT-2, RapidEye, and WorldView-2. A linear regression analysis using the simulated satellite single band as the variable was applied to assess the potentials of the three satellite sensors for N nutritional status diagnosis. In addition, vegetation indices (VIs) were* *computed based on the simulated satellite wavebands. The results indicated the NIR1 band was most important for estimating all the N status indicators. According to the R^2 values, the regression models based on the simulated WorldView-2 wavebands had the highest performance for biomass, plant N uptake (PNU), and nitrogen nutrition index (NNI) estimations, followed by the ones based on the RapidEyewavebands, at each of the three stages. The red-edge band improved biomass, PNU, and NNI estimations at all three stages, especially at the early PI and SE stages. Biomass and PNU were best estimated using data across the stages while NNI and plant nitrogen concentration (PNC) were best estimated at the HE stage. For VI analysis, 30-40% biomass variability was explained using the Chlorophyll Index (CI) at thePI and SE stages. Likewise, 39-52% PNU variability was explained using the CI based on the FORMOSAT-2wavebands. The best VIs based on RapidEye and WorldView-2 wavebands explained 53-64% biomass variability, and 62-65% PNU variability.For the NNI estimation, the N planar domain index (NPDI) based on WorldView-2 wavebands and MERIS terrestrial chlorophyll index (MTCI) based on RapidEyewavebands explained 14-26% more variability.*

Keywords.*Satellite remote sensing, red-edge band, nitrogen status diagnosis，nitrogen nutrition index, vegetation index，rice.*

The authors are solely responsible for the content of this paper, which is not a refereed publication. Citation of this work：

Huang,S., Miao, Y., Yuan, F., Gnyp, M.L., Yao, Y., Cao, Q., Lenz-Wiedemann, V.&Bareth, G. (2016).Potential improvement in rice nitrogen status monitoring using RapidEye and WorldView-2 satellite remote sensing. In Proceedings of the 13th International Conference on Precision Agriculture (unpaginated, online). St. Louis, Missouri, USA. International Society of Precision Agriculture.

1. Introduction

Nearly two third of the Chinese population depends on rice (*Oryza sativa* L.) as main food, which makes rice as one of the most important staple food crops(Dawe et al., 2000). Nitrogen (N) is very important in rice production, because it is a key element for chlorophyll constitution. Chlorophyll content affects photosynthesis rate, which thereby affects biomass production and yield largely. Thus, in-season monitoring of the crop N status can provide a guidance for in-season site-specific N management (Dobermann et al., 2003).

The rice crop area in Northeast China has increased rapidly during the past decade, and this region has become more and more important for China's food security and sustainable development(Zhao et al., 2013).Although real time N status monitoring technologies using handheld chlorophyll meter and active crop canopy sensors have been used to improve rice N management in this region (Yao et al., 2012; Cao et al., 2013), these technologies are still very time consuming and not suitable for large scale rice farming applications. Satellite remote sensing is more promising and efficient for large scale crop growth monitoring. Huang et al. (2015) used the FORMOSAT-2 satellite images to diagnose rice N status in Northeast China and proposed a nitrogen nutrition index (NNI)-based strategy for guiding topdressing N application.

Most of the satellite remote sensing images have four traditional wavebands-blue, green, red and near infrared (NIR). The commonly used satellite-based vegetation indices (VIs) were mostly red- and green-band based, such as normalized difference vegetation index (NDVI) and ratio vegetation index (RVI). These VIs may saturate under moderate-to-high biomass conditions at later growth stages (Thenkabail et al., 2000; Mutanga and Skidmore, 2004).To solve this problem, many new VIs were developed. The red-edge based VIs were proven to be sensitive to crop canopy chlorophyll and N variation and could improve the agronomic parameters estimation, because red-edge-based spectral indices can overcome the saturation problems as reported with NDVI (Van Niel and McVicar, 2004; Nguy-Robertson et al., 2012).In 2008, RapidEye was launched and was the first commercial satellite including the red-edge band with 6.5 m spatial resolution. After this, WorldView-2 was launched in October of 2009 and supplies very high spatial resolution imagery (2 m for multispectral wavebands image and 0.5 m for panchromatic image). It has eight wavebands, also including a red-edge band.

So far, little has been reported on the potential of improving rice N status monitoring using these two new satellite images as compared with the commonly used four band satellite images like FORMOSAT-2. Therefore, the objective of this study was 1) to compares the application potential of the satellite FORMOSAT-2, RapidEye, and WorldView-2 by 2) evaluate the N indicators estimation by using the vegetation indices based on their band settings, respectively, and 3) to improve the predictive power for aboveground biomass, PNC, PNU, and NNI estimation. Considering the challenge of collecting these three satellite images together at several key rice growth stages, this study used proximal hyperspectral reflectance data to simulate the wavebands of these three satellite images.

2. Materials and methods

2.1 Study area and study sites

The study area is located at the Qixing Farm in the Sanjiang Plain, Heilongjiang Province, Northeast China. The Sanjiang Plain used to be a wild natural wetland formed by the alluvium of three river systems - Heilong River, Songhua River, and Wusuli River. This area has a typical cool-temperate sub-humid continental monsoon climate. During the growing season (April-October), the average rainfall is about 400 mm, which accounts for approximately 70% of yearly precipitation. The mean annual temperature is about 2 ^{o}C (Wang and Yang, 2001).

Two sites were selected to conduct 10 N rate experiments in Qixing Farm. Rice has been planted in

Site 1 (47°15'52"N, 132°39'05"E) since 1992 while Site 2 (47°13'59"N, 132°38'50"E) started rice planting in 2002.

2.2 Experimental design

The N rate experiments were conducted in 2008, 2009, and 2011 at the study sites involving a Japonica 11 leaf cultivar rice named Kongyu 131 (Table 1). All of the experiments adopted randomized complete block design with three or four replications. The nitrogen fertilizer was applied in three splits for Experiments 1-6: 40-45% as basal application before transplanting, 20-30% at the tillering stage, and 30-35% at the stem elongation stage. For Experiments 7-10, N fertilizers were applied in two splits: 60% as basal application and 40% at tillering stage. In each experiment, sufficient phosphate (45-60 kg P_2O_5 ha^{-1}) and potash (90-105 kg K_2O ha^{-1}) fertilizers were applied to ensure sufficient P and K nutrients. All the P fertilizers were applied as basal fertilizers before transplanting. The K fertilizers were applied in two splits, with 50% as basal fertilizer and 50% as panicle fertilizer at the stem elongation stage.

2.3 Plant sampling and analysis

Plant samples were collected at several critical growth stages, including the panicle initiation (PI), stem elongation (SE), heading (HE) stages. Sampling time and date were different from each experiments and detailed information was listed in Table 1. In all sampling process, the samples were harvested using the same protocol. All the plant samples were rinsed with water and the roots were removed. Then the samples were separated into leaves, stems and panicles (for samples collected at and after heading stage). The separated samples were put into the oven at 105°C for half an hour for deactivation of enzymes, and then dried at 70-80 °C until constant weight. After being weighed, the samples were ground into powder and sub-samples were sieved using 1 mm sieves for plant N concentration (PNC) analysis using the standard Kjeldahl-N method. The plant N uptake (PNU) was determined by multiplying PNC with dry biomass.

Table 1. Details of the nitrogen rate experiments conducted from 2008 to 2012 in Jiansanjiang, Northeast China.

Experiment	Site	Year	Cultivar	N Application Rates (kg ha^{-1})	Transplanting/Harvesting Date	Sampling Stage
1	1	2008	Kongyu 131	0, 35, 70, 105, 140	29-May / 21-September	PI, SE, HE
2	2	2008	Kongyu 131	0, 35, 70, 105, 140	13-May / 22-September	PI, SE, HE
3	1	2009	Kongyu 131	0, 35, 70, 105, 140	24-May / 27-September	SE, HE
4	2	2009	Kongyu 131	0, 35, 70, 105, 140	20-May /27-September	PI,SE, HE
5	1	2011	Kongyu 131	0, 70, 100, 130,160	17-May / 21-September	PI
6	1	2011	Longjing 21	0, 70, 100, 130, 160	19-May / 21-September	PI
7	1	2008	Kongyu 131	0, 23, 45, 68, 91	29-May / 21-September	HE
8	2	2008	Kongyu 131	0, 23, 45, 68, 91	13-May / 22-September	HE
9	1	2009	Kongyu 131	0, 23, 45, 68, 91	24-May / 27-September	SE, HE
10	2	2009	Kongyu 131	0, 23, 45, 68, 91	20-May / 27-September	SE, HE

PI stands for panicle initiation stage; SE stands for stem elongation stage; HE stands for heading stage.

For the Nitrogen Nutrition Index (NNI) calculation, the critical nitrogen concentration (N_c) was calculated by following equation developed for rice in this region based on data from N rate experiments conducted in this region from 2008 to 2013:

$$N_c = 2.77W^{-0.34} \quad (1)$$

where N_c is the critical N concentration (%) in the aboveground biomass and W is the shoot dry weight expressed in t ha^{-1}. For aboveground biomass larger than 1 t ha^{-1}, the N_c was calculated by the above equation, otherwise the N_c was set to 2.77%.

The NNI was defined as the ratio of the actual PNC (N_a) and the N_c. NNI is a convenient and reliable indicator for diagnosing crop N status (Lemaire et al., 2008). If N_a is greater than N_c (NNI>1), it indicates an over-supply of N while the opposite is true if N_a is smaller than N_c (NNI<1). A NNI value of 1 indicates an optimal N supply (Lemaire et al., 2008).

2.4Field spectral measurements and resampling

The rice canopy reflectance was collected using portable hyperspectral instruments FieldSpec3 (Analytical Spectral Devices Inc., Boulder, Co, USA) for Experiment 1-4, 7-10, and ASD QualitySpec Pro (Analytical Spectral Devices Inc., Boulder, Co, USA) for Experiment 5, 6. The spectrometer of QualitySpec Pro collects reflectance wavelength between 350 to 1800 nm with 1.2 nm interval for the spectral region of 350-1000 nm and 2 nm interval for the spectral region 1000-1800 nm. And the FieldSpec 3 collects reflectance wavelength between 350 to 2500 nm with 1.2 nm interval for the 350-1000 nm spectral region and 2 nm interval for the 1000-2500 nm spectral region. The canopy reflectance was obtained at sunny cloudless condition at midday (9:00 a.m.-1:00 p.m.). In addition, the measurements were taken 0.3 m above the canopy with 25^{o} field of view. The reflectance was calibrated by measuring a barium sulfate ($BaSO_4$) reference panel at least every 10-15 min. Five-six times scanning were taken randomly in each plot, and then were averaged as the plot reflectance.

The FORMOSAT-2 (F2), RapidEye (RY), and WorldView-2 (WV2) satellite systems are carried on satellites that all run on sun-synchronous orbit but with different orbit altitudes. The FORMOSAT-2 is a daily revisit satellite launched on May of 2004 and collects images at the same local hour with a constant observation angle for the same site (Chern et al., 2006). The spectral range of WV2 covers from 400 nm to 1040 nm including costal (400-450 nm), blue (450-510 nm), green (510-581 nm), yellow (582-625 nm), red (630-690 nm), red-edge (705-745 nm), near-infrared 1(770-895 nm), near-infrared 2 (860-1040 nm) wavebands. RapidEye also includes a red-edge band in addition to the traditional four bands. The band settings information and other properties for those three satellite sensors were listed in Table 2.

Table 2. Comparison the launched time, orbit altitude, spectral, multispectral and panchromatic spatial resolution, revisit time, and swath width of the FORMOSAT-2, RapidEye, and WorldView-2 satellite sensors.

Properties	FORMOSAT-2	RapidEye	WorldView-2
Type	sun-synchronous	sun-synchronous	sun-synchronous
Launched time	May-04	Aug-08	Oct-09
Orbit altitude (km)	891 km	620	770 km
Spatial Resolution for multispectral image (m)	8	6.5	2
Spatial Resolution for panchromatic image (m)	2	-#	0.5
Revisit time (Day)	1	1	1.1
Swath width (km)	24	80	16.4
Band settings	450-520 nm (Blue: F_b) 520-600 nm (Green: F_g) 630-690 nm (Red: F_r) 760-900 nm (Near-infrared: F_nir1)	440-510 nm (Blue: R_b) 520-590 nm (Green: R_g) 630-685 nm (Red: R_r) 690-730 nm (Red-edge: R_re) 760-900 nm (Near-infrared: R_nir1)	400-450 nm (Coastal: W_c) 450-510 nm (Blue: W_b) 510-581 nm (Green: W_g) 585-625 nm (Yellow: W_y) 630-690 nm (Red: W_r) 705-745 nm (Red-edge: W_re) 770-895 nm (Near-infrared1: W_nir1) 860-1040 nm (Near-infrared2: W_nir2)

#The RapidEye satellite doesn't collect the panchromatic imagery.

The hyperspectral data were resampled to simulate the band settings of the three satellite sensors following the band equivalent reflectance theory. The hyperspectral data were resampled to simulated FORMOSAT-2, RapidEye, and WorldView-2 wavebands based on the spectral response functions as shown in Equation 2:

$$r_i = \sum_{\lambda u_i}^{\lambda l_i} r(\lambda)\, \varphi_i(\lambda) \Big/ \sum_{\lambda u_i}^{\lambda l_i} \varphi_i(\lambda) \tag{2}$$

In which, r_i stands for the reflectance of Band i; ,λl_i is the starting wavelength of Band i,λu_i is the termination wavelength of Band i; $r(\lambda)$ is the reflectance value at Wavelengthλ,$\varphi_i(\lambda)$ is the band response function of Band i at wavelengthλ. The band response function data of FORMOSAT-2 was provided by the National Space Organization of Taiwan (NSPO),and the corresponding data of RapidEye and WorldView-2 were supplied by the software ENVI 4.8 (ENVI, Boulder, Colorado, USA).

2.5Data analysis

The vegetation indices (VIs) listed in Table 3 have been calculated using SPSS V.20.0 (SPSS, Chicago, Illinois, USA) to estimate the N status indicators of the Experiment 1-10. Simple linear regression was used to determine the relationship between each spectral index and N status indicators. The coefficient of determination (R^2) was used to compare the performance of the vegetation indices. The coefficients of determination of the relationships between single bands of FORMOSAT-2 (F2), RapidEye (RY), WorldView-2 (WV2) and the N status indicators were also performed in SPSS.

Table 3. Vegetation indices evaluated in this study for estimating rice N status indicators.

Vegetation Index	Formula	Satellite sensors	Reference
Ration vegetation index (RVI)	NIR/R	F2, RY, WV2	Jordan, 1969
Green chlorophyll index (CI)	NIR/G-1	F2, RY, WV2	Gitelson et al., 2005
Normalized difference vegetation index (NDVI)	(NIR-R)/(NIR+R)	F2, RY, WV2	Rouse et al., 1974
Green normalized difference vegetation index (GNDVI)	(NIR-G)/(NIR+G)	F2, RY, WV2	Gitelson and Merzlyak,1996
Optimized soil-adjusted vegetation index (OSAVI)	(1+0.16)*((NIR–R) /(NIR+R+0.16))	F2, RY, WV2	Rondeaux et al., 1996
Modified chlorophyll absorption in reflectance index (MCARI)	((NIR–R)–0.2(R–G))*(NIR/R)	F2, RY, WV2	Daughtry et al., 2000
Triangular Vegetation Index (TVI)	0.5*(120(NIR–G)–200(R–G))	F2, RY, WV2	Broge and Leblanc, 2000
Modified transfromed chlorophyll absorption in reflectance index (TCARI)	3*((NIR-R)-0.2(NIR-G)(NIR/R))	F2, RY, WV2	Haboudane et al., 2002
MCARI/OSAVI	MCARI/OSAVI	F2, RY, WV2	Haboudane et al., 2002
TCARI/OSAVI	TCARI/OSAVI	F2, RY, WV2	Haboudane et al., 2002
Red-edge chlorophyll index (CI_re)	NIR/Re-1	RY, WV2	Gitelson et al., 2005
Nromalizeddiffernce red-edge index (NDRE)	(NIR-Re)/(NIR+Re)	RY, WV2	Fitzgerald et al.,2010
MERIS terrestrial chlorophyll index (MTCI)	(NIR-Re)/(Re-R)	RY, WV2	Dash and Curran,2004
Canopy chlorophyll content index (CCCI)	(NDRE-NDREmin) /(NDREmax-NDREmin)	RY, WV2	Fitzgerald et al., 2010
Nitrogen planar domain index (NDPI)	(CI_re-CI_re_min) /(CI_re_max-CI_re_min)	RY, WV2	Clarke et al., 2001
Red-edge-based optimized soil-adjusted vegetation index (OSAVI_re)	(1+0.16)*((NIR–Re) /(NIR+Re+0.16))	RY, WV2	Wu et al., 2008
Red-edge-based modified chlorophyll absorption in reflectance index (MCARI_re)	((NIR–Re)–0.2(Re–G))*(NIR/Re)	RY, WV2	Wu et al., 2008
Red-edge-based Triangular Vegetation Index (TVI_re)	0.5*(120(NIR–G)–200(Re–G))	RY, WV2	Broge and Leblanc, 2000
Red-edge-based modified transfromed chlorophyll absorption in reflectance index (TCARI_re)	3*((NIR-Re)-0.2(NIR-G)(NIR/Re))	RY, WV2	Wu et al., 2008
MCARI_re/OSAVI_re	MCARI_re/OSAVI_re	RY, WV2	Wu et al., 2008
TCARI_re/OSAVI_re	TCARI_re/OSAVI_re	RY, WV2	Wu et al. , 2008

3. Results

3.1Variation of the N status indicators

The descriptive statistics of the AGB, PNC, PNU, and NNI at the PI, SE, and HE stages were listed in Table 4. The biomass increased from 1.11 t ha^{-1} at the PI stage to 1.78 t ha^{-1} at the SE stage, and to 6.28 t ha^{-1} at the HE stag while PNU also increased from 27.53 kg N ha^{-1} to 40.13 kg N ha^{-1} at the SE stage, and increased to 103.34 kg N ha^{-1} at the HE stage. The PNC decreased from 2.47 % at the PI stage to 2.36 % at the SE stage, and further decreased shapely from the SE stage to 1.62% at the HE stage, affected by the “dilution effect” described by Plénet and Lemaire (1999). The average NNI was 0.96 at the PI stage, which slowly increased from 1.01 at the SE stage to 1.09 at the HE stage. The standard deviation of biomass, PNC, PNU, and NNI increased from the PI to HE stage, which indicated the difference grew lager and lager between different N rate treatments with the development of the growth stages. The coefficients of variation (CV) for biomass and PNU increased from the PI to SE stage, and peaked at the SE stage, but decreased from the SE to HE stage. In addition, CV for PNC and NNI increased with the development of the growth stages, especially at the HE, which indicated the PNC and NNI maybe easier to be remotely estimated after heading stage. These results also indicated the importance of using NNI for N status diagnosis, rather than other indicators.

Table 4. Descriptive statistics of the measured aboveground biomass, nitrogen concentration, plant N uptake, and NNI for the model estimation and validation across PI, SE and HE stages.

Stage		AGB(t ha^{-1})	PNC(%)	PNU(kg N ha^{-1})	NNI
PI	n	57	57	57	57
	Min	0.2	2.16	4.39	0.8
	Max	2.19	3	59.32	1.29
	Mean	1.11	2.47	27.53	0.96
	SD	0.5	0.17	12.71	0.11
	CV	45.02	6.97	46.17	11.4
SE	n	92	92	92	92
	Min	0.57	1.53	14.76	0.77
	Max	3.96	3.15	91.82	1.47
	Mean	1.78	2.36	40.13	1.01
	SD	0.88	0.36	16.96	0.14
	CV	49.36	15.11	42.26	13.74
HE	n	98	98	98	98
	Min	3.44	0.83	44.59	0.53
	Max	9.92	2.18	205.64	1.63
	Mean	6.28	1.62	103.34	1.09
	SD	1.49	0.28	36.2	0.24
	CV	23.75	17.06	35.03	21.97

n, number of observations; SD, standard deviation of the mean; CV, coefficient of variation; the unit for CV was in %.

3.2 Single band analysis

The simulated NIR1band was best correlated with AGB, PNU, and NNI for all three satellites at the PI stage, which explained 31-32% model variability for AGB, 29-30% for PNU, 22% for NNI, respectively (Fig. 1a, e, g). TheNIR2 band of WV2 was the second rank for AGB and PNU estimations. In visible wavelengths, the red band performed the best than others, while the green band performed the worst. The simulated red-edge band of WV2 was more significantly correlated to AGB, PNU, and NNI than RY at the PI stage(Fig. 1a, e, g). However, the PNC was hard to be estimated using the single simulated wavebands at the PI stage (Fig. 1c). The analysis results of the relationship between simulated single wavebands and N status indicators as mentioned in this study for the SE stage were similar with the PI stage (data not show). Compared to the PI stage, the performance of NIR1 and NIR2 decreased while the R^2 of visible wavelengths increased at the HE stage (Fig. 1b, f, h). The PNC and NNI were better estimated, while the AGB was harder to be estimated at the HE stage (Fig. 1d, h). The red band of RY and WV2, and the yellow band of WV2 reached highest R^2, which was 0.28-0.29 for PNC, 0.31-0.32 for PNU, and 0.34 for NNI estimation, respectively (Fig. 1d, f, h). Contrary to the PI stage, the simulated red-edge band of RY was more significantly correlated to AGB, PNU, and NNI than WV2 at the HE stage (Fig. 1b, f, h).

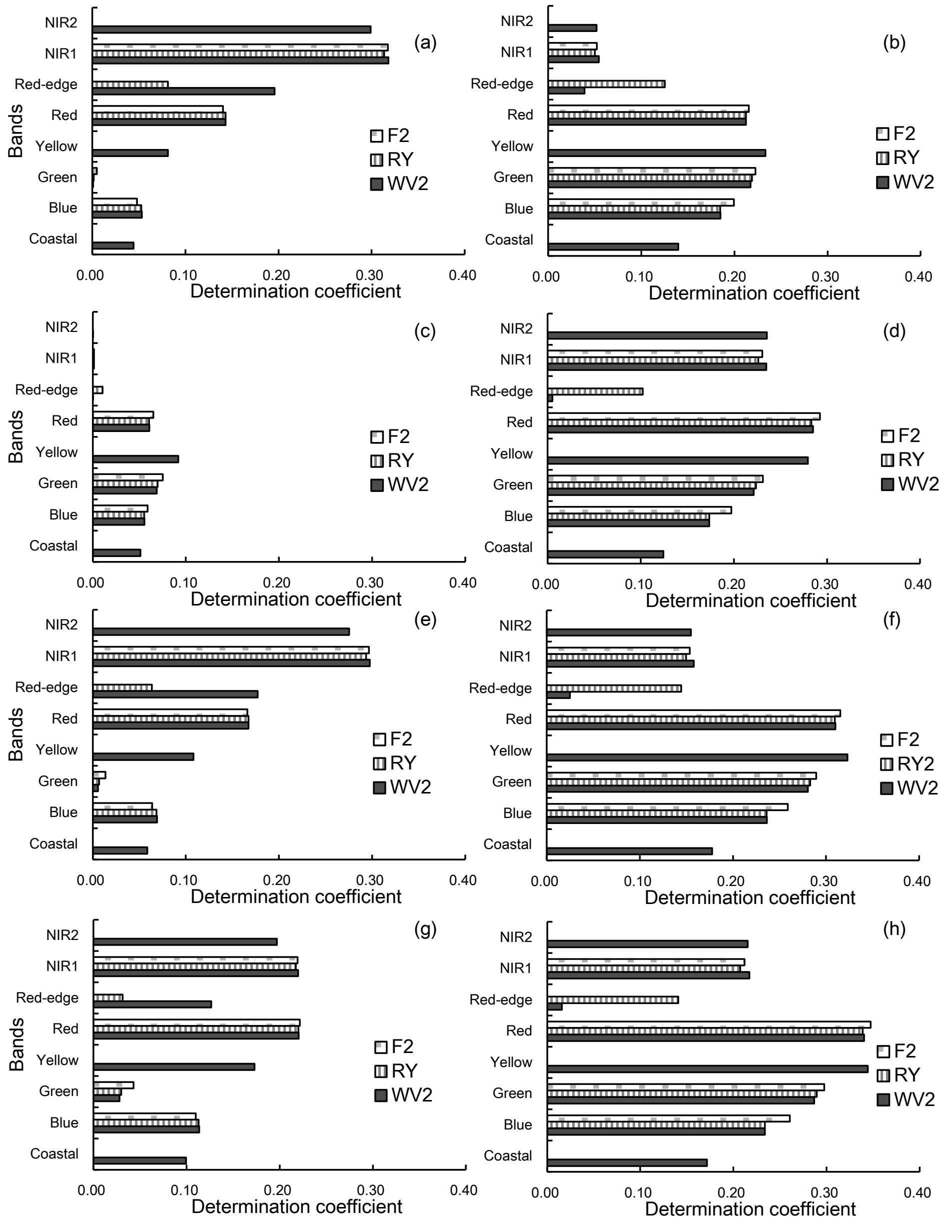

Fig. 1. Coefficient of determination (R^2) for the relationships between reflectance of simulated FORMOSAT-2, RapidEye, WorldView-2 wavebands and AGB at the PI stage (a), HE stage (b), PNC at the PI (c), PNC at the HE (d), PNU at the PI (e), PNU at the HE (f), NNI at the PI (g), NNI at the HE (h).

3.3 Correlation between nitrogen indicators and vegetation index

To evaluate the effects of wavelength for different satellites and growth stages on the relationships between vegetation indices and N status indicators, we calculated the same VIs based on the same wavebands of different satellites (Table 3), and then analyzed the linear regression correlation for Panicle Initiation, Stem Elongation, and Heading growth stages. The top 5 VIs were listed in Tables 5-6.

Most of VIs performed significantly better than single wavebands (Table 5-6). The PNC was still hard to be estimated, but the R^2 of the best performance also has doubled than the best single band. For F2, the R^2 of the best performed VI slightly increased compared to the best single band. In general, the red-edge indices of RY and WV2 performed better than the non-red-edge VIs of F2 for estimating the AGB, PNU, and NNI at the PI and SE stages (Table 5 and 6). At the PI and SE stages, the red-edge index MTCI of RY and WV2 performed the best for estimating AGB and PNU, with R^2 ranged from 0.53 to 0.64 and from 0.60 to 0.64, respectively. This was followed by the red-edge indices CCCI, NDPI, CI_re, NDRE, and TVI_re, which all achieved better model results than non-red-edge based indices (Table 5 and 6). At the HE stage, the performance of red-edge-based indiceswas similar to the non-red-edge indices for AGB and NUP estimations. The top 5 indices of WV2 were similar to those of RY. The red-edge-based indices of WV2 performed better than RY except for CCCI at all three stages, which might be caused by the different red-edge band settings between the two satellite sensors (Table 2).

Table 5. The top 5 coefficients of determination (R2) for the relationships between vegetation indices based on the wavebands of FORMOSAT-2, RapidEye, WorldView-2 and aboveground biomass, plant N concentration (PNC) at the PI, SE, HE stages, respectively.

Panicle Initiation Stage		Stem Elongation Stage		Heading Stage	
Index	AGB (t ha^{-1})	Index	AGB (t ha^{-1})	Index	AGB (t ha^{-1})
F2-CI	0.39**	F2-GNDVI	0.41**	F2-CI	0.28**
F2-GNDVI	0.35**	F2-OSAVI	0.41**	F2-GNDVI	0.27**
F2-MCARI/OSAVI	0.33**	F2-NDVI	0.41**	F2-RVI	0.21**
F2-TCARI/OSAVI	0.34**	F2-CI	0.40**	F2-NDVI	0.20**
F2-RVI	0.33**	F2-TVI	0.39**	F2-TCARI/OSAVI	0.18**
RY-MTCI	0.64**	RY-MTCI	0.53**	RY-MTCI	0.28**
RY-CCCI	0.61**	RY-CCCI	0.51**	RY-CCCI	0.28**
RY-NDPI	0.59**	RY-NDPI	0.50**	RY-NDPI	0.28**
RY-CI_re	0.46**	RY-CI_re	0.47**	RY-CI_re	0.28**
RY-NDRE	0.43**	RY-NDRE	0.46**	RY-NDRE	0.28**
WV2-NDPI	0.65**	WV2-MTCI	0.57**	WV2-NDPI	0.30**
WV2-MTCI	0.62**	WV2-NDPI	0.54**	WV2-MTCI	0.30**
WV2-TVI_re	0.57**	WV2-CI_re	0.51**	WV2-CI_re	0.30**
WV2-CI_re	0.54**	WV2-NDRE	0.50**	WV2-NDRE	0.30**
WV2-NDRE	0.53**	WV2-TVI_re	0.47**	WV2-CCCI	0.30**
Index	PNC (%)	Index	PNC (%)	Index	PNC (%)
F2-CI	0.02	F2-NDVI	0.06*	F2-CI	0.53**
F2-GNDVI	0.02	F2-GNDVI	0.04	F2-GNDVI	0.52**
F2-RVI	0.02	F2-OSAVI	0.03	F2-NDVI	0.46**
F2-TCARI/OSAVI	0.02	F2-CI	0.01	F2-RVI	0.44**
F2-TCARI	0.02	F2-RVI	0.01	F2-TCARI/OSAVI	0.42**
RY-TCARI_re/OSAVI_re	0.07	RY-TCARI_re	0.09**	RY-CI_re	0.57**
RY-GNDVI	0.03	RY-NDVI	0.06*	RY-MTCI	0.56**
RY-CI_re	0.02	RY-NDRE	0.05*	RY-NDPI	0.56**
RY-NDPI	0.02	RY-MTCI	0.04	RY-NDRE	0.55**
RY-MTCI	0.02	RY-GNDVI	0.04	RY-TCARI_re/OSAVI_re	0.55**
WV2-GNDVI	0.03	WV2-MTCI	0.07*	WV2-OSAVI_re	0.57**
WV2-CI_re	0.02	WV2-NDVI	0.06*	WV2-CI_re	0.56**
WV2-NDPI	0.02	WV2-NDRE	0.05*	WV2-MTCI	0.56**
WV2-NDRE	0.02	WV2-GNDVI	0.04	WV2-NDRE	0.56**
WV2-CI	0.02	WV2-CI_re	0.04	WV2-NDPI	0.55**

**. Correlation is significant at the 0.01 level; *. Correlation is significant at the 0.05 level.

The results of Table 5indicated that PNC was not significantly related to most of the vegetation indices at the PI and SE stages. At the HE stage, the indices significantly improved estimation of PNC with R^2 ranging from 0.42 to 0.57. The red-edge based indices performed slightly better compared to the red- and green-based indices at the HE stage. The vegetation index F2-TCARI/OSAVI、 RY-TCARI_re/OSAVI_re improved PNC estimation at HE stage.

Table 6 indicated the red-edge indices slightly improved the NNI estimation compared to the non-red-edge indices, especially the index MTCI, NDPI, CI_re, and NDRE. At HE stage, the red edge index NDPI, CI_re, MTCI, NDRE performed the best (R^2=0.60-0.62), and better than CI (R^2=0.58-0.59) and GNDVI (R^2=0.57) which were the best performed non-red-edge indices.

Table 6 The top 5 coefficients of determination (R2) for the relationships between vegetation indices based on the wavebands of FORMOSAT-2, RapidEye, WorldView-2 and plant N uptake (PNU), nitrogen nutrition index (NNI) at the PI, SE, HE stages, respectively.

Panicle Initiation Stage		Stem Elongation Stage		Heading Stage	
Index	PNU (kg ha^{-1})	Index	PNU (kg ha^{-1})	Index	PNU (kg ha^{-1})
F2-CI	0.39**	F2-CI	0.52**	F2-CI	0.50**
F2-GNDVI	0.35**	F2-TVI	0.52**	F2-GNDVI	0.48**
F2-TCARI/OSAVI	0.34**	F2-GNDVI	0.50**	F2-RVI	0.40**
F2-RVI	0.33**	F2-OSAVI	0.50**	F2-NDVI	0.39**
F2-MCARI/OSAVI	0.33**	F2-MCARI/OSAVI	0.49**	F2-TCARI/OSAVI	0.36**
RY-MTCI	0.62**	RY-MTCI	0.64**	RY-NDPI	0.52**
RY-CCCI	0.59**	RY-CCCI	0.62**	RY-CI_re	0.52**
RY-NDPI	0.58**	RY-NDPI	0.61**	RY-MTCI	0.51**
RY-CI_re	0.46**	RY-CI_re	0.57**	RY-TCARI_re	0.51**
RY-NDRE	0.43**	RY-TVI_re	0.56**	RY-TCARI_re/OSAVI_re	0.51**
WV2-NDPI	0.63**	WV2-NDPI	0.65**	WV2-CI_re	0.62**
WV2-MTCI	0.60**	WV2-MTCI	0.64**	WV2-NDPI	0.61**
WV2-TVI_re	0.54**	WV2-TVI_re	0.61**	WV2-MTCI	0.61**
WV2-CI_re	0.53**	WV2-CI_re	0.60**	WV2-NDRE	0.61**
WV2-NDRE	0.52**	WV2-NDRE	0.59**	WV2-OSAVI_re	0.61**
Index	NNI	Index	NNI	Index	NNI
F2-CI	0.35**	F2-TCARI	0.34**	F2-CI	0.58**
F2-TCARI/OSAVI	0.32**	F2-TCARI/OSAVI	0.33**	F2-GNDVI	0.57**
F2-RVI	0.31**	F2-MCARI	0.33**	F2-NDVI	0.48**
F2-GNDVI	0.31**	F2-MCARI/OSAVI	0.32**	F2-RVI	0.47**
F2-MCARI/OSAVI	0.29**	F2-CI	0.30**	F2-TCARI/OSAVI	0.44**
RY-MTCI	0.44**	RY-MCARI_re	0.35**	RY-NDPI	0.61**
RY-NDPI	0.44**	RY-CCCI	0.34**	RY-CI_re	0.61**
RY-CI_re	0.38**	RY-TCARI	0.34**	RY-MTCI	0.61**
RY-CCCI	0.36**	RY-MTCI	0.33**	RY-NDRE	0.60**
RY-NDRE	0.36**	RY-MCARI_re/OSAVI_re	0.33**	RY-TCARI_re/OSAVI_re	0.60**
WV2-MTCI	0.41**	WV2-NDPI	0.37**	WV2-CI_re	0.62**
WV2-CI_re	0.41**	WV2-MCARI_re	0.36**	WV2-NDPI	0.61**
WV2-NDRE	0.41**	WV2-TVI_re	0.36**	WV2-MTCI	0.61**
WV2-NDPI	0.40**	WV2-TCARI	0.34**	WV2-NDRE	0.61**
WV2-TVI_re	0.38**	WV2-TCARI/OSAVI	0.33**	WV2-OSAVI_re	0.61**

**. Correlation is significant at the 0.01 level; *. Correlation is significant at the 0.05 level.

Tables 5 and 6 indicated that some VIs were among the Top 5 VIs for all the three stages. In Fig. 2, the scatter plots show the best performed VIs for AGB, PNU, and NNI. The CI based on green reflectance was the best one for FORMOSAT-2. MTCI and NDPI based on red-edge reflectance were the best one for RapidEye, and WorldView-2, respectively. Those three VIs did not saturate at high biomass condition (Fig. 2).

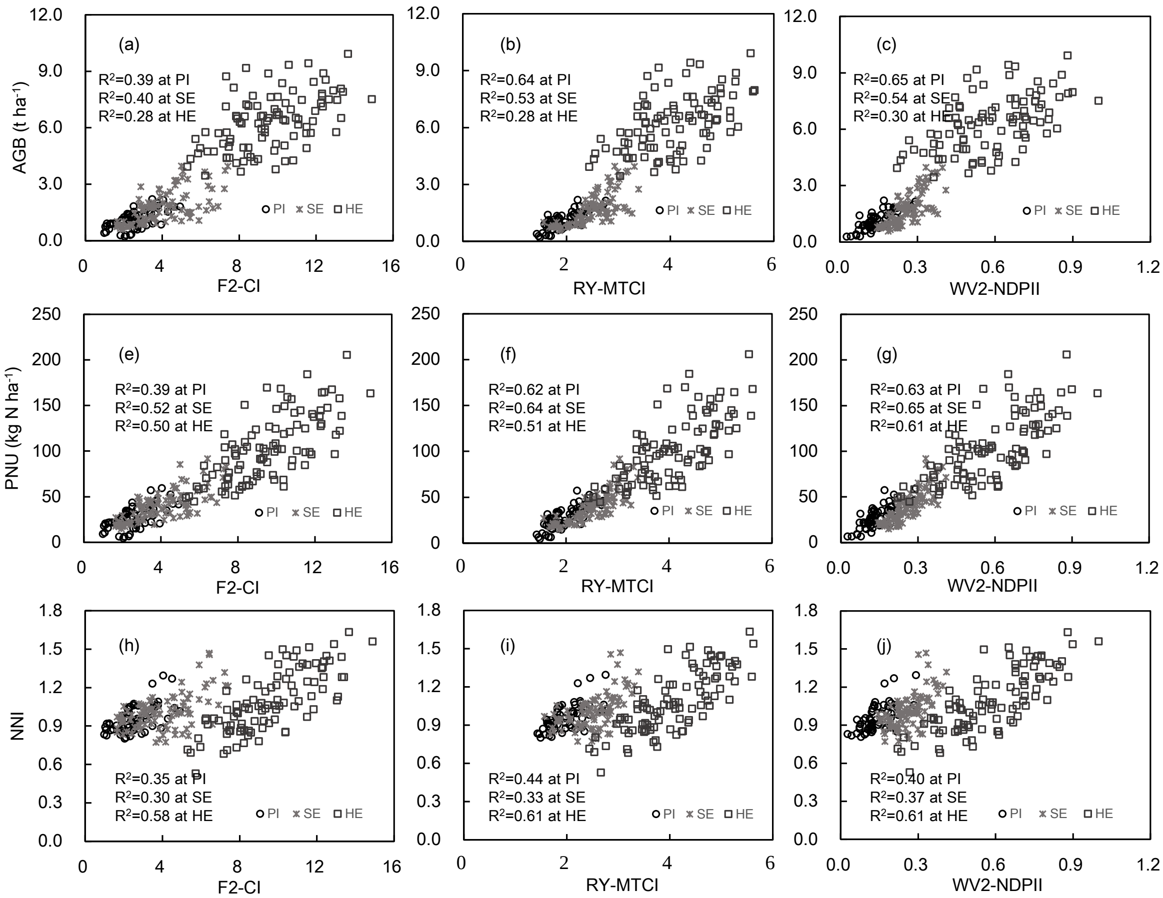

Fig.2. Relationships between FORMOSAT2-CI (a), RapidEye-MTCI (b), WorldView2-NDPI and aboveground biomass, FORMOSAT 2-CI (e), RapidEye-MTCI (f), WorldView 2-NDPI (g) and nitrogen N uptake, FORMOSAT 2-CI (h), RapidEye-MTCI (i), WorldView 2-NDPI (j) and NNI at the PI, SE, and HE stage.

4. Discussion

Growth stages have significant impacts on estimating N status parameters. The AGB and PNU increase with the advancement of growth stages, and accordingly have positive correlations with N nutritional status. Our results indicated that, most of the VIs estimated AGB and PNU better than PNC at the PI and SE stages, but estimated PNC better than AGB at the heading stage. Yu et al. (2013) also found the VIs performed better for estimating PNC after heading. NNI is a dimensionless parameter, which is defined as the ratio of actual PNC with critical PNC. NNI increased with increasing N rates, and this trend remains consistent during the growth cycle (Gastal et al., 2001; Farruggia et al., 2004). The stage-specific analysis was suitable for NNI estimation. The NNI-based map can directly be used to guide in-season topdressing N applications (Huang et al., 2015; Cilia et al., 2014).

At early stage, the soil background may influence the vegetative reflectance at red band. Although the red band-based VIs (like NDVI and RVI) were the most commonly used indices in N status estimation, they are easily influenced by soil background. In addition, the NDVI saturated at high biomass condition. When the red band was replaced by red-edge band to from new VIs such as NDRE and CI_re, they significantly improved the estimation results compared to NDVI and RVI (Table 5 and 6).This was because the red-edge reflectance was proven to be highly correlated with chlorophyll (Cho and Skidmore, 2006; Clevers et al., 2002), responsive to variation in LAI or biomass (Haboudane et al., 2002;Gnypet al., 2014), and insensitive to background effects (Zarco-Tejada et al., 2004). The red-edge vegetation indices-MTCI, CCCI, and NDPI were proven to be highly correlated with AGB and PNU (Li et al., 2012；Yu et al., 2013; Shiratsuchi et al., 2011; Ramoeloet al., 2012; Li et al., 2014).In our study, the MTCI, CCCI, and NDPI of RY, and MTCI, NDPI of WV2 had better relationships with AGB (Table 5), PNU (Table 6), and NNI (Table 6), which conforms to previous researchers.

Over the last few years, a number of studies have re-sampled field spectra data to simulate the wavebands of existing or planned satellite sensors and to evaluate their application potential (Li et al., 2014; Ramoelo et al., 2012; Dong et al., 2015). However, the results were not validated using actual satellite images. Random forest regression was proven to be an effective method for evaluating the robustness of resampled models on real WorldView-2 images (Mutanga et al., 2015).It can be used to evaluate the findings of this study in future research.

Conclusion

This study simulated the band settings of FORMOSAT-2, RapidEye, and WorldView-2 satellite images to evaluate their potentials to improve rice N status estimation. The single band correlation, analysis indicated the NIR1 band was the most important for estimating these N status indicators. In addition, the red-edge band improved biomass, PNU, and NNI estimations at all three stages, especially at the early PI and SE stages. For VI analysis, the best performed red-edge-based VIs explained 53-64% biomass variability and 62-65% PNU variability, compared to 30-40% biomass and 39-52% PNU variability using the Chlorophyll Index (CI) at the PI and SE stages. For the NNI estimation, the N planar domain index (NPDI) based on WorldView-2 wavebands and MERIS terrestrial chlorophyll index (MTCI) based on RapidEye wavebands explained 14-26% more variability.

Acknowledgements

We thank the staff of Jiansanjiang Bureau of Agricultural Land Reclamation, Qixing Farm and Jiansanjiang Institute of Agricultural Research for their support. We also would like to thank Kang Yu, Lei Gao, and Hongye Wang for their field work and spectral measurements collection. This study was financially supported by the Sino-Norwegian Cooperative SINOGRAIN project (CHN-2152, 14-0039).

References

Broge, N.H., Leblanc, E. (2000). Comparing prediction power and stability of broadband and hyperspectral vegetation indices for estimation of green leaf area index and canopy chlorophyll density. *Remote Sensing of Environment,* 76, 156-172.

Cao, Q.; Miao, Y.; Wang, H.; Huang, S.; Cheng, S.; Khosla, R.; Jiang, R. (2013). Non-destructive estimation of rice plant nitrogen status with Crop Circle multispectral active canopy sensor. *Field Crops Research*, 154, 133-144.

Chern, J.S., Wu, A.M., Lin, S.F. (2006). Lesson learned from FORMOSAT-2 mission operations. *Acta Astronautica*, 59, 344-350.

Cho, M.A., Skidmore, A.K. (2006). A new technique for extracting the red edge position from hyperspectral data: The linear extrapolation method. *Remote Sensing of Environment*, 101(2), 181-193.

Cilia, C., Panigada, C., Rossini, M., Meroni, M., Busetto, L., et al. (2014). Nitrogen status assessment for variable rate fertilization in maize through hyperspectral imagery. *Remote Sensing*, 6, 6549-6565.

Clarke, T.R., Moran, M.S., Barnes, E.M., Pinter, P.J., Qi, J. (2001). Planar domain indices: A method for measuring a quality of a single component in two-component pixels. In Proc. IEEE International Geoscience and Remote Sensing Symposium (pp. 1279-1281). Sydney, Australia.

Clevers, J.G.P.W., De Jong, S.M., Epema, G.F., Van Der Meer, F.D., Bakker, W.H., Skidmore, A.K., Scholte, K.H. (2002). Derivation of the red edge index using theMERIS standard band setting. *International Journal of Remote Sensing*, 23 (16), 3169–3184.

Dash, J., Curran, P.J. (2004). The MERIS terrestrial chlorophyll index. *International Journal of Remote Sensing,* doi: 10.1080/0143116042000274015.

Daughtry, C.S.T., Walthall, C.L., Kim, M.S., Colstoun, E.B., McMurtrey III, J.E. (2000). Estimating corn leaf chlorophyll concentration from leaf and canopy reflectance. *Remote Sensing of Environment*, 74, 229-239.

Dawe, D (2000). The contribution of rice research to poverty alleviation. *Studies in Plant Science*, 7, 3-12.

Dobermann, A., Witt, C., Abdulrachman, S., Gines, H.C., Nagarajan, R. et al. (2003). Estimating indigenous nutrient supplies for site-specific nutrient management in irrigated rice. *Agronomy Journal*, 95(4), 924-935.

Dong, T., Meng, J., Shang, J., Liu, J., Wu, B. (2015). Evaluation of chlorophyll-related vegetation indices using simulated Sentinel-2 data for estimation of crop fraction of absorbed photosynthetically active radiation. *IEEE Journal of Selected Topics in Applied Earth Observations and Remote Sensing,* 8(8), 4049-4059.

Farruggia, A., Gastal, F., Scholefield, D. (2004). Assessment of the nitrogen status of grassland. *Grass and Forage Science*, 59(2): 113-120.

Fitzgerald, G., Rodriguez, D., O'Leary, G. (2010). Measuring and predicting canopy nitrogen nutrition in wheat using a spectral index-The canopy chlorophyll content index (CCCI). *Field Crops Research*, 116(3), 318-324.

Gastal, F., Farruggia, A., Hacquet, J. (2001). The nitrogen nutrition index of grass can be evaluated through determination of N concentration of upper leaves. In Proc. of the 2001 11th Nitrogen Workshop (pp. 9-12). Reims, France.

Gitelson, A.A., Kaufman, Y.J., Merzlyak, M.N. (1996). Use of a green channel in remote sensing of global vegetation from EOS-MODIS. *Remote Sensing of Environment*, 58, 289-298.

Gitelson, A.A., Viña, A., Ciganda, V., Rundquist, D.C., Arkebauer, T.J. (2005). Remote estimation of canopy chlorophyll content in crops. *Geophysical Research Letters*, doi:10.1029/2005GL022688.

Gnyp, M.L., Miao, Y., Yuan, F., Ustin, S.L., Yu, K. et al. (2014). Hyperspectral canopy sensing of paddy rice aboveground biomass at different growth stages. *Field Crops Research*, 155, 42-55.

Haboudane, D., Miller, J.R., Tremblay,N., Zarco-Tejada, P.J., Dextraze, L. (2002). Integrated narrow-band vegetation indices for prediction of crop chlorophyll content for application to precision agriculture. *Remote Sensing of Environment*, 81, 416-426.

Huang, S., Miao, Y., Zhao, G., Yuan, F., Ma, X., et al. (2015). Satellite Remote Sensing-Based In-Season Diagnosis of Rice Nitrogen Status in Northeast China. *Remote Sensing*, 7(8), 10646-10667.

Jordan, C.F. (1969). Derivation of leaf-area index from quality of light on the forest floor. *Ecology*, 663-666.

Lemaire, G., Jeuffroy, M.H., Gastal, F. (2008). Diagnosis tool for plant and crop N status in vegetative stage: Theory and practices for crop N management. *European Journal of Agronomy*, 28, 614-624.

Li, F, Mistele,B., Hu, Y., Yue, X., Yue, S., et al. (2012). Remotely estimating aerial N status of phenologically differing winter wheat cultivars grown in contrasting climatic and geographic zones in China and Germany. *Field Crops Research*, 138, 21-32.

Li, F., Miao, Y., Feng, G., Yuan, F., Yue, S., et al. (2014). Improving estimation of summer maize nitrogen status with red edge-based spectral vegetation indices. *Field Crops Research,* 157, 111-123.

Mutanga, O., Adam, E., Adjorlolo, C., Abdel-Rahman, E.M. (2015). Evaluating the robustness of models developed from field spectral data in predicting African grass foliar nitrogen concentration using WorldView-2 image as an independent test dataset. International Journal of Applied Earth Observation and Geoinformation, 34, 178-187.

Mutanga, O., Skidmore, A.K. (2004) Narrow band vegetation indices overcome the saturation problem in biomass estimation. *International Journal of Remote Sensing*, 25(19), 3999-4014.

Nguy-Robertson, A., Gitelson, A., Peng, Y., Viñaet, A., Arkebauer, T., Rundquist, D. (2012). Green leaf area index estimation in maize and soybean: combining vegetation indices to achieve maximal sensitivity. *Agronomy Journal*, 104(5), 1336-1347.

Plénet, D., Lemaire, G. (1999). Relationships between dynamics of nitrogen uptake and dry matter accumulation in maize crops. Determination of critical N concentration. *Plant and Soil,* 216(1-2), 65-82.

Ramoelo, A., Skidmore, A.K., Cho, M.A., Schlerf, M., Mathieu, R., Heitkönig, I.M.A. (2012). Regional estimation of savanna grass nitrogen using the red-edge band of the spaceborne RapidEye sensor. *International Journal of Applied Earth Observation and Geoinformation*, 19: 151-162.

Rondeaux, G., Steven, M., Baret, F. (1995). Optimization of soil-adjusted vegetation indices. *Remote Sensing of Environment*, 55(2): 95-107.

Rouse, J.W., Has, R.H., Schell, J.A., Deering, D.W. (1974). Monitoring vegetation systems in the great plains with ERTS. Washington, DC, NASA.

Shiratsuchi, L., Ferguson, R., Shanahan, J., Adamchuk, V., Rundquist, D., Marx, D.,Slater, G. (2011). Water and nitrogen effects on active canopy sensor vegetation indices. *Agronomy Journal*, 103, 1815–1826.

Thenkabail, P.S., Smith, R.B., Pauw, E.D. (2000). Hyperspectral vegetation indices and their relationships with agricultural crop characteristics. Remote Sensing of Environment, 71, 158-182.

Van Niel, T.G., McVicar, T.R. (2004). Current and potential uses of optical remote sensing in rice-based irrigation systems: a review. *Australian Journal of Agricultural Research*, 55 (2),155–185.

Wang, Y., Yang, Y. (2001). Effects of agriculture reclamation on hydrologic characteristics in the Sanjiang Plain. *Chinese Geographical Science*, 11, 163-167.

Wu, C., Niu, Z., Tang, Q., Huang, W. (2008). Estimating chlorophyll content from hyperspectral vegetation indices: Modeling and validation. Agricultural and Forest Meteorology, 148(8), 1230-1241.

Yao, Y.; Miao, Y.; Huang, S.; Gao, L.; Zhao, G.; Jiang, R. et al. (2012). Active canopy sensor-based precision N management strategy for rice. *Agronomy for Sustainable Development*, 32, 925-933.

Yu, K., Li, F., Gnyp, M.L., Miao, Y., Bareth, G., Chen,X. (2013). Remotely detecting canopy nitrogen concentration and uptake of paddy rice in the Northeast China Plain. *ISPRS Journal of Photogrammetry Remote Sensing*, 78, 102-115.

Zarco-Tejada, P.J., Miller, J.R., Morales, A., Berjon, A., Aguera, J. (2004). Hyperspectral indices and model simulation for chlorophyll estimation in open-canopy tree crops. *Remote Sensing of Environment*, 90 (4), 463–476.

Zhao, G.; Miao, Y.; Wang, H.; Su, M.; Fan, M.; Zhang, F.; Jiang, R.; Zhang, Z.; Liu, C.; Liu, P.; Ma, D. (2013). A preliminary precision rice management system for increasing both grain yield and nitrogen use efficiency. *Field Crops Research*, 154, 23-30.